DALTON

Electron self-exchange and cross-reaction studies on wild-type *Clostridium pasteurianum* rubredoxin and its Val-8→Glu variant†

Sang-Choul Im, Hua-Yun Zhuang-Jackson, Takamitsu Kohzuma, Panayotis Kyritsis, William McFarlane * and A. Geoffrey Sykes *

Department of Chemistry, The University of Newcastle, Newcastle upon Tyne NE1 7RU, UK

The electron self-exchange rate constant (k_{ese}) for recombinant *Clostridium pasteurianum* rubredoxin in the Fe^{II} and Fe^{III} forms, referred to here as Rd_{red} and Rd_{ox}, has been determined. Using NMR spectroscopy the procedure involves monitoring the perturbation introduced by increasing concentrations of the Rd_{ox} form on the longitudinal and transverse relaxation times of hyperfine-shifted ^1H NMR signals of Rd_{red}. A second-order rate constant k_{ese} (25 °C) of 1.6×10^5 M^{-1} s^{-1} has been obtained at pH 6.5, $I = 0.100$ M (NaCl). Similar measurements carried out with the molecular variant in which valine-8 is replaced by glutamate (Val8Glu) give a significantly smaller k_{ese} value of 4.7×10^3 M^{-1} s^{-1}. The effect of the negatively charged Glu-8, adjacent to the surface-exposed Cys-9 and Cys-42 residues of the Fe active site, suggests a close Fe–Fe approach of ≈12 Å for electron exchange. The reduction potential *vs.* NHE of rubredoxin by cyclic and square-wave voltammetry (using a promotor) determined as −81 mV is pH invariant, but that of Val8Glu (−73 mV at pH ≥ 6.5) depends on pH, with pK_a 6.2 for Rd_{red} and 5.8 for Rd_{ox}. Rate constants from cross-reaction studies involving the oxidation of Rd_{red} by *Pseudomonas aeruginosa* azurin and cytochrome c_{551} have also been determined using the stopped-flow method, and kinetic data analysed in the framework of the Marcus theory. Azurin in particular with its close to electroneutral surface has been successfully used as a redox partner in other inter-protein cross-reaction studies. However calculated electron self-exchange rate constants k_{ese} for the Rd_{red}–Rd_{ox} couple average 35 M^{-1} s^{-1}, and are $> 10^3$ smaller than the value determined by NMR spectroscopy, indicating the possible involvement of a different reaction site for these reactions.

Rubredoxins (Rd) are non-haem iron proteins found in a variety of bacteria.[1–3] Those isolated from anaerobic organisms have 46 to 54 amino acids ($M_r \approx 6000$) and one iron atom per molecule.[4] Only in the case of *Desulfovibrio gigas*, is information about the function of rubredoxin as an electron-transfer agent beginning to emerge.[5–7] In contrast, another type of Rd from *Pseudomonas oleovorans*, containing two Fe centres per molecule, is an essential electron carrier in the enzymatic system associated with fatty acid and hydrocarbon hydroxylation processes.[8]

Rubredoxin from *Clostridium pasteurianum* was the first to be isolated,[9] and its structure from high-resolution X-ray crystallography shows the Fe atom to be tetrahedrally co-ordinated by four cysteines at positions 6, 9, 39 and 42 of the sequence.[10] There are four other crystal structures of rubredoxins.[11–14] The overall folding of the molecule occurs around an extensive core of aromatic residues in a barrel-like arrangement having six antiparallel sections. The $Fe(Cys)_4$ unit can be viewed as lying on top of the barrel, with the Fe *ca.* 6 Å from the surface of the molecule.[10] The estimated charge balance on *C. pasteurianum* Rd_{ox} is −10 at pH ≈ 7 arising from Asp/Glu residues (−13), Lys (+4) and the $Fe(Cys)_4$ cluster (−1). The surface residues close to the active site are mainly hydrophobic.

Two oxidation states, Rd_{red} and Rd_{ox}, in which the iron atom is high-spin d^6 Fe^{II} ($S = 2$) and d^5 Fe^{III} ($S = \frac{5}{2}$) respectively, are available to the rubredoxins. The kinetic properties associated with the redox interconversion have received little attention largely because amounts of the protein obtained from natural sources are small. From one study so far reported a high intrinsic redox reactivity has been suggested.[15,16] The structural changes associated with redox interconversion give an average lengthening of the Fe–S bonds of 0.035 Å, as determined for the crystal structure of *Pyrococcus furiosus* rubredoxin.[14] A lengthening (again small at 0.06 Å) was also deduced from EXAFS analysis on *C. pasteurianum* rubredoxin in its two oxidation states.[17] The bond lengths and changes observed are similar to those observed for model complexes.[18]

Electron-transfer properties of the rubredoxins are relevant to their function and warrant more detailed consideration. With the amounts of protein now available from an expression system it has been possible to determine the self-exchange rate constant (k_{ese}) by measuring the relaxation times of hyperfine shifted NMR signals for different ratios of $[Rd_{red}]/[Rd_{ox}]$. Such rate constants are of fundamental importance reflecting inherent electron-transfer properties of the protein in the absence of a thermodynamic driving force. Other recent studies in which k_{ese} values have been reported are for Type 1 blue copper,[19] haem[20] and high potential Fe–S proteins.[21] Protein–protein cross-reaction studies in which k_{ese} values can be calculated using the Marcus theory have also been carried out.[19] In order to obtain information about the site of electron transfer studies on the Val8Glu variant are also reported. In previous applications of the NMR method one reactant in the exchange process has been paramagnetic and the other diamagnetic. The present studies are the first example in which both participants are paramagnetic, and the successful use of equations depends upon the relaxation times of relevant protons in the reduced and oxidised forms being sufficiently different.

Experimental

Preparations

Rubredoxins. Recombinant *Clostridium pasteurianum* rubredoxin isolated from *Escherichia coli* K38/pGP1-2/pTRD1, according to a previously described procedure,[22] was

† *Non-SI unit employed:* M = mol dm^{-3}.

generously provided by Dr. J.-M. Moulis. The gene bearing the GTA→GAA mutation encoding the Val8Glu variant was prepared by two successive rounds of PCR on plasmid pTRD1, using a previously established method.[23] The mutagenic oligonucleotide had the following sequence: 5'aaatatatccacat-Tctgtacatgtatac, with the changed base in upper case. The purification of Val8Glu followed the procedure used for recombinant wild-type rubredoxin.

Purification of protein was by fast protein liquid chromatography (FPLC) using a mono-Q anion-exchange column and 20 mM tris(hydroxymethyl)aminoethane (Tris)–HCl buffer, pH 7.0, with a linear 0 to 1.0 M NaCl ionic strength gradient. The Rd_{ox} protein eluted at 38–39% of 1.0 M NaCl, with a UV/VIS absorption peak ratio A_{490}/A_{280} of 0.43. The UV/VIS absorption bands λ/nm (10^{-3} ε/M^{-1} cm^{-1}) for *C. pasteurianum* Rd_{ox} are at 490 (8.85), 380 (10.8) and 280 (21.3), and for Rd_{red} at 333 (6.3), 311 (10.8) and 275 (24.8).[9] No alteration in the UV/VIS spectrum was observed due to the Val 8Glu change. Protein Rd_{ox} concentrations were determined from the absorbance at 490 nm (ε = 8850 M^{-1} cm^{-1}). In order to obtain Rd_{red} sodium dithionite was added to the protein solution in a Miller-Howe glove-box (O_2 < 2 ppm).

Other proteins. The single Type 1 blue copper protein azurin and cytochrome c_{551} were isolated from *Pseudomonas aeruginosa* as previously described.[24] The final purification of azurin was by Pharmacia FPLC mono-S cation-exchange column, using a linear 0 to 1 M NaCl gradient in 20 mM acetate buffer pH 4.7. Pure ACu^{II} protein has a UV/VIS absorption peak ratio A_{280}/A_{625} of 1.67–1.72. Concentrations of ACu^{II} were determined from the absorbance at 625 nm (ε 5200 M^{-1} cm^{-1}).[25] The purification of cytochrome c_{551} was achieved by FPLC mono-Q, anion-exchange column using a linear 0 to 1 M NaCl gradient in 20 mM Tris–HCl buffer, pH 8.0. The reduced Fe^{II} cytochrome c_{551} protein has a UV/VIS absorption peak ratio A_{551}/A_{280} of 1.10. Concentrations were determined from the absorbance at 416 nm ($\varepsilon = 6.25 \times 10^4$ M^{-1} cm^{-1}). A prominent peak at 551 nm ($\varepsilon = 2.86 \times 10^4$ M^{-1} cm^{-1}) is observed for the Fe^{II} protein.[24,25] At pH *ca.* 7 azurin ACu^{II} and cytochrome c_{551} Fe^{III} have low charge balance of zero and −2 respectively, and there are no regions of high charge on their surfaces.[26]

Buffers. For electrochemical studies at pH 4.6 sodium acetate trihydrate (pK_a = 4.88), for experiments in the range pH 5.0–6.5, 2-(morpholino)ethanesulfonic acid (Mes, pK_a = 6.10) with NaOH added, and in the range pH 7.0–8.0 Tris (pK_a 8.08) with HCl added were used (20 mM). For NMR studies wild-type rubredoxin was exchanged into 99.9% deuteriated 20 mM phosphate, and the Val8Glu variant was exchanged into 95% D_2O + 5% H_2O deuteriated 20 mM phosphate buffer, both solutions at pH 6.5, I = 0.100 M (NaCl). All buffers were from Sigma Chemical Co. The pH of solutions was measured on a Radiometer PHM 62 meter. After the NMR experiments the pH was checked using a narrow Russell CMAWL/3.7/180 pH probe. No corrections to the measured pH were made for deuterium isotope effects.

Electrochemistry measurements

Cyclic voltammetry and square-voltammetry were carried out using a standard three-electrode configuration of gold, Ag–AgCl and platinum as working, reference and auxiliary electrodes respectively. The gold electrode was hand polished using in turn 0.03 and 0.015 μm aqueous aluminium oxide (BDH) slurries of buff as polishing material (Böehler), and cleaned by sonication for ≈30 s. The gold electrode was modified using solutions of 4,4'-dithiodipyridine (dtpy) or 2-(diethylamino)ethanethiol [2-(diethylamino)ethyl mercaptan, deaet] as promotors (Sigma). Both promotors give positively charged surfaces suitable for interaction with the negatively charged protein.[27] Samples were transferred to the working compartment of the electrochemical microcell (≈500 μL) in the glove-box. Cyclic and square-wave voltammetry were carried out with a Princeton Applied Research model 173 potentiostat. Interfacing was to an IBM PC computer with software from EG&G. All measurements were carried out at 25 °C with pulse height 25 mV, a frequency of 12 Hz and potential increments of 2 mV in the square-wave voltammetry. For cyclic voltammetry a scan rate of 20 mV and scan increments of 1 mV were used. Reduction potentials have also been determined by redox titration methods using a procedure previously described.[28]

Solutions for NMR studies

Protein samples were exchanged into the required buffer by ultrafiltration using an Amicon cell. To obtain reduced protein, aliquots of 0.1 M $Na_2S_2O_4$ in 99.9% D_2O were added. The dithionite was standardised using $[Fe(CN)_6]^{3-}$ by UV/VIS spectrophotometry. Oxidised protein Rd_{ox} was introduced at this stage in the glove box. The amounts of Rd_{red} and Rd_{ox} were checked by UV/VIS spectrophotometry, and ≈0.5 cm^3 of solution transferred into the NMR tube and sealed with a rubber cap. After NMR measurements had been completed solutions were again transferred to a UV/VIS spectrophotometer cell in the glove box and the absorbance checked (differences < 3%).

NMR spectra

All one-dimensional ^1H NMR spectra were acquired at 500.14 MHz on a Bruker AMX 500 spectrometer at temperatures of 25 and 35 °C (± 1 °C) controlled by an air stream. Free induction decays were accumulated into 16 K data points and transformed into 32 K data points after zero-filling. The residual HDO resonance was suppressed by presaturation at its resonance frequency. All chemical shifts are expressed in parts per million (ppm) relative to the water peak at δ 4.8. The inversion recovery sequence (180°–T_D–90°–acquire) was used for T_1 measurements. The T_2 values were determined from peak widths at half-height ($\nu_{\frac{1}{2}}$) using the relationship $\nu_{\frac{1}{2}} = (\pi T_2)^{-1}$. The calculation of k_{ese} depends upon determining the effect of the increased paramagnetism of Rd_{ox} (high spin d^5) upon the relaxation behaviour of Rd_{red} (high spin d^6) resonances, and the relaxation times of specific protons were therefore determined for solutions containing different proportions of the two forms of the protein.

Approximate solutions of the equations linking the relaxation times of two exchanging species A and B with the individual relaxation properties of each have been derived,[29] and are valid when the rate of exchange (k) is either significantly faster or slower than the individual relative relaxation rates in the two species. In the former case (fast exchange) $kc \gg T_{ip}^{-1}$, where c is the total concentration of A and B, and the relaxation times of the exchanging species are independent of k. In the latter case (slow exchange), the condition translates into $kc \ll T_{ip}^{-1}$. In each case T_{ip} is $|T_{iA}^{-1} - T_{iB}^{-1}|$ (i = 1 or 2), and for a dilute solution in which [B] ≫ [A] equation (1) holds,

$$T_i^{-1} = T_{iB} + k[A] \quad (1)$$

where T_{iB} are the relaxation times of the more concentrated species B.[29] In the present context A corresponds to oxidised and B to reduced protein, and it is important to establish that the slow-exchange regime applies to the protons whose resonances are used to determine k_{ese}. When one species is diamagnetic and the other paramagnetic, as in the case of the blue copper proteins, then this condition depends effectively upon T_i in the paramagnetic form being sufficiently short, and this will generally be fulfilled for protons sufficiently close to the

Table 1 Electrochemical data of rubredoxin at 25 °C, all potentials *vs.* the normal hydrogen electrode (NHE), $I = 0.100$ M (NaCl)

(*a*) Square-wave voltammetry for wild-type Rd_{ox}–Rd_{red}

pH	$E^{o\prime}$/mV	Promoter
5.0	−79	deaet
5.0	−67	dtpy
6.0	−81	deaet
7.0	−83	deaet
7.0	−86	dtpy
8.0	−80	deaet

(*b*) Cyclic voltammetry for wild-type Rd_{ox}–Rd_{red}

pH	$E_{\frac{1}{2}}$/mV	Promoter
5.0	−69	dtpy
5.0	−82	deaet
6.0	−85	deaet
7.0	−83	deaet
7.0	−83	dtpy
8.0	−84	deaet

(*c*) Square-wave voltammetry for the Val8Glu variant Rd_{ox}–Rd_{red}

pH	$E^{o\prime}$/mV	Promoter
4.6	−48	deaet
5.1	−50	deaet
5.5	−56	deaet
5.7	−56	deaet
6.0	−62	deaet
6.5	−71	deaet
7.0	−73	deaet
8.0	−75	deaet

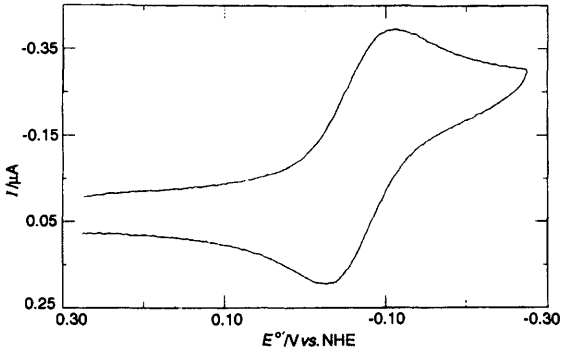

Fig. 1 Cyclic voltammogram (≈25 °C) for wild-type rubredoxin, Rd_{ox} (3.5×10^{-4} M) at pH 5.0 with 4,4′-dithiodipyridine as promoter at a gold electrode, $I = 0.100$ M (NaCl)

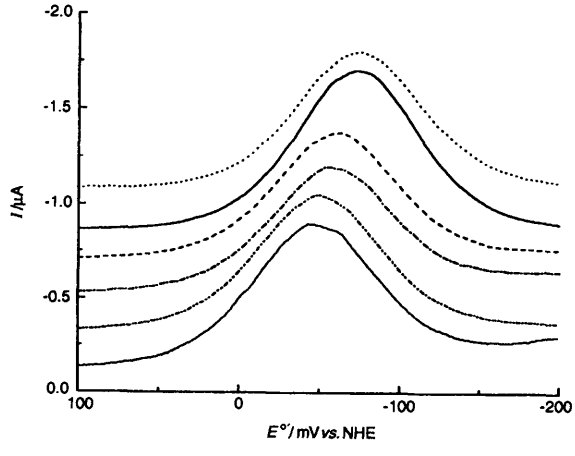

Fig. 2 Square-wave voltammograms (≈25 °C) for the Val8Glu rubredoxin variant ($\approx 1.0 \times 10^{-5}$ M) at pH's in descending order 8.0, 7.0, 6.0, 5.5, 5.1 and 4.6, $I = 0.100$ M (NaCl)

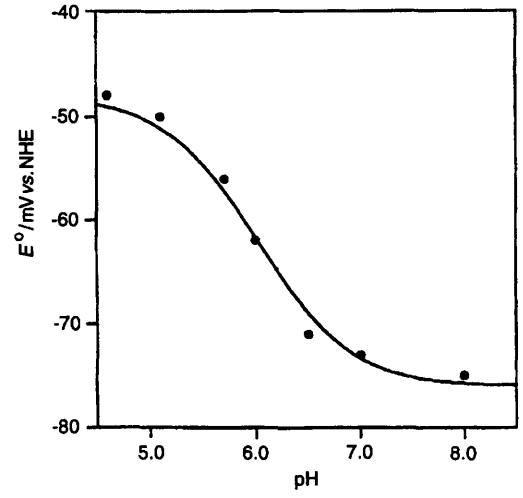

Fig. 3 The variation of $E^{o\prime}$ (*vs.* NHE) for the Val8Glu rubredoxin variant with pH at 25 °C, with fitted line according to equation (2), $I = 0.100$ M (NaCl)

metal. However, in the present circumstances, with both states paramagnetic, it may be harder to satisfy the slow-exchange condition as (*a*) for protons very close to the metal the resonances may be unobservable in either form, and (*b*) T_{iA} and T_{iB} may be insufficiently different.

It should also be borne in mind that since both Rd_{red} and Rd_{ox} are paramagnetic the changes in T_i are smaller than when one state is diamagnetic. This has a significant effect upon the precision of measurements, but is not expected to alter our overall conclusions.

Protein–protein cross reactions

All kinetic runs were monitored on a Dionex D-110 stopped-flow spectrophotometer at 25.0 ± 0.1 °C and $I = 0.100 \pm 0.001$ (NaCl). The spectrophotometer was interfaced to an IBM PC/AT-X computer for data acquisition using software from On-Line Instruments Systems (Bogart, GA, USA). All quoted rate constants are an average of at least five determinations using the same made-up solutions. It was necessary to use pH = 7.0 for those studies since the previously determined k_{ese} values for the azurin and cytochrome c_{551} couples were at this pH [see equation (7) below].

Results

Reduction potentials

These were determined for the Rd_{ox}–Rd_{red} couple by direct electrochemical measurements using in turn two promoters. Both square-wave and cyclic voltammetry methods were employed, Table 1. Voltammograms were well defined, Figs. 1 and 2. No effects of pH were observed for the wild-type Rd_{ox}–Rd_{red} in the range 5.0–8.0, and we conclude that $E^{o\prime}$ is −81 ± 2 mV, which compares with an earlier value by spectrophotometric titration of −57 mV.[9] Similar experiments on Val8Glu from square-wave voltammetry (limited amounts of variant) gave $E^{o\prime}$ values −73 ± 2 mV at pH ≥ 6.5, which decreased to −48 ± 1 at pH ≤ 4.6, Table 1. From a fit of data to the relationship (2),[30] where E_0 is the reduction potential of the

$$E^{o\prime} = E_0 - 0.060 \log \frac{K_a(\text{ox}) + [H^+]}{K_a(\text{red}) + [H^+]} \qquad (2)$$

fully protonated protein, acid dissociation pK_a values assigned to Glu-8 are 6.2 ± 0.1 (Rd_{red}) and 5.8 ± 0.1 (Rd_{ox}), Fig. 3. Potentiometric measurements involving titration of Rd samples (80 μM) with $S_2O_4^{2-}$ and $[Fe(CN)_6]^{3-}$ at pH 8.2 (personal

Table 2 Rate constants k_1 and k_2 (25 °C) derived from an analysis of T_1 and T_2 data for wild-type Rd[a] and the Val8Glu variant[b] at pH 6.5, I = 0.100 M (NaCl)

δ/ppm	$[Rd_T]$/mM	$10^{-5}k_1{}^a$/M^{-1} s^{-1}	$10^{-5}k_2{}^a$/M^{-1} s^{-1}	$10^{-5}k_1{}^b$/M^{-1} s^{-1}	$10^{-5}k_2{}^b$/M^{-1} s^{-1}
200[c]	1.23		≈40		
11.8	0.30		1.5		
	0.43[d]		0.72		
	1.32		1.2		
	1.40				0.019
10.4	0.30		2.1		
	0.43[d]		2.0		
	1.23	0.92	1.6		
	1.32		1.7		
	1.40			0.036	0.047
	1.80	0.59	2.2		
10.2	0.30		2.2		
	0.43[d]		2.0		
	1.23	1.20	2.9		
	1.32		1.5		
	1.40			0.035	0.088
	1.80		2.4		
−1.1	0.30		2.6		
	0.43[d]		2.0		
	1.23	0.034	1.2		
	1.32		1.5		
	1.40			0.030	
	1.80		0.75		
	0.30		6.8		
−2.4	0.43[d]		3.2		
	1.23	5.07	2.5		
	1.32		1.3		
	1.40			0.017	0.17
	1.80		1.3		
−3.6	1.23		2.1		
−4.2	1.23		2.1		

[a] Wild-type Rd (99% D_2O). [b] Val8Glu variant of Rd (95% D_2O + 5% H_2O). [c] Cysteine β-CH_2 peak, ref. 29. [d] At 22 °C.

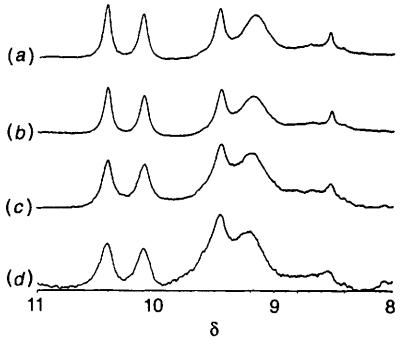

Fig. 4 Selected NMR spectra at 25 °C of wild-type rubredoxin showing the effect of Rd_{ox} [0, 0.12, 0.37 and 0.49 mM for (*a*)–(*d*) respectively] on the line widths, total concentration $[Rd_T]$ = 1.23 mM, pH 6.5 (20 mM phosphate), I = 0.100 M (NaCl)

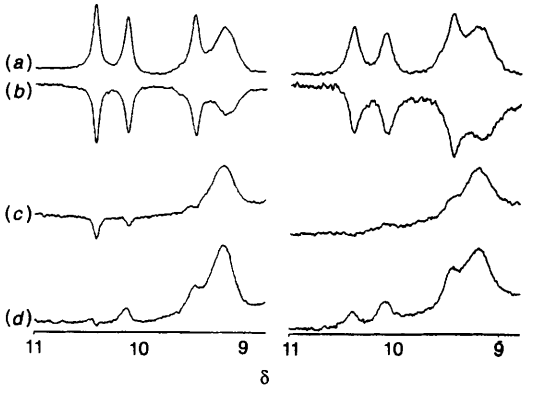

Fig. 5 Selected NMR spectra from inversion recovery experiments on fully reduced (left), and partly oxidised $[Rd_{ox}]$ = 5.2 × 10^{-4} M (right) wild-type protein used in T_1 measurements, $[Rd_T]$ = 1.23 mM, pH 6.5 (20 mM phosphate), I = 0.100 M (NaCl). The spectra were obtained with a 180°–T_D–90° pulse sequence, and T_D at 2000, 0.5, 6 and 10 ms for (*a*)–(*d*) respectively

communication Dr. J.-M. Moulis) do not give any marked differences in potentials determined for wild-type protein and the Val8Glu variant. Potentials determined as −90 ± 5 mV for wild-type protein are in agreement with those in Table 1.

Determination of k_{ese}

For the wild-type protein the protons studied in detail were those which have signals at δ 200,[31] 11.8, 10.4, 10.2, −2.4, −3.6 and −4.2 in the reduced protein at pH 6.5, Table 2. The corresponding resonances in the oxidised protein were not observed under our conditions of measurement. For the Val8-Glu variant the protons resonating at δ 11.8, 10.4, 10.2 and −1.1 were used. Spin–lattice (T_1) and spin–spin (T_2) relaxation times were determined at pH 6.5, for solutions containing different proportions of oxidised Rd at several total concentrations of Rd between 0.3 and 1.8 mM, and at 25 and 35 °C. Fig. 4 shows parts of spectra from samples of the wild-type protein containing different proportions of Rd_{ox}, and indicates that resonances at δ 10.4 and 10.2 are broadened by the presence of Rd_{ox}. Fig. 5 shows inversion recovery experiments on fully reduced and partially oxidised samples of the wild-type protein, from which it is evident that for the δ 10.4 and 10.2 resonances, spin–lattice relaxation is faster in the presence of Rd_{ox}. Comparable spectra to those of Fig. 4 were obtained for the Val8Glu variant as shown in Fig. 6.

Values of T_1 and T_2 at 25 and 35 °C for the protons studied at different concentrations of Rd_{ox} were plotted against $[Rd_{ox}]$. Fig. 7 shows typical T_1 and T_2 plots. Tables 2 and 3 list rate constants derived from the slopes of such plots.

Table 3 Rate constants k_1 and k_2 (35 °C) derived from an analysis of T_1 and T_2 data for wild-type Rd[a] and the Val8Glu variant[b] at pH 6.5, I = 0.100 M (NaCl)

δ/ppm	$[Rd_T]$	$10^{-5}\,k_1{}^a/M^{-1}\,s^{-1}$	$10^{-5}\,k_2{}^a/M^{-1}\,s^{-1}$	$10^{-5}\,k_1{}^b/M^{-1}\,s^{-1}$	$10^{-5}\,k_2{}^b/M^{-1}\,s^{-1}$
10.4	1.30			0.037	0.022
	1.50	1.0	3.6		
10.2	1.30			0.092	0.066
	1.50	1.9	3.1		
−1.1	1.30			0.030	
	1.50	0.73	0.97		
−2.4	1.50	3.1	0.25		
−3.6	1.30			No peak	No peak
	1.30		8.9		
−4.2	1.35				
	1.50		2.1		

[a] Wild-type Rd (99% D_2O). [b] Val8Glu variant of Rd (95% D_2O + 5% H_2O).

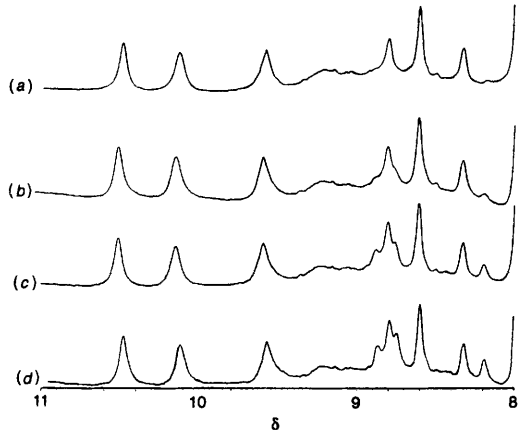

Fig. 6 Selected NMR spectra (25 °C) for the Val8Glu variant of Rd_{red} (1.4 mM) with Rd_{ox} 0, 0.21, 0.42 and 0.56 mM for (*a*)–(*d*) respectively at pH 6.5 (20 mM phosphate), I = 0.100 M (NaCl)

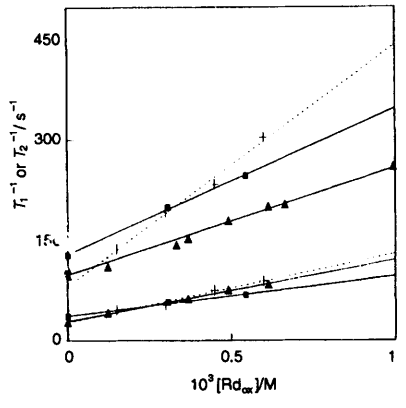

Fig. 7 Plots of T_1^{-1} (lower three) and T_2^{-1} (upper three) against $[Rd_{ox}]$ using the δ 10.4 peak in 20 mM phosphate solution at pH 6.5 with $[Rd_T]$ = 1.8 (■) and 1.3 mM (▲), I = 0.100 M (NaCl). The temperature was adjusted to 25 °C (■, ▲) and 35 °C (+)

Owing to the different distances from the paramagnetic centre and other factors, different protons may be associated with different exchange rate regimes. Fig. 8 shows plots of $[Rd_T](T_{2ox}^{-1} - T_{2red}^{-1})/[Rd_{ox}]$ against $[Rd_T]$ for selected proton resonances of the wild-type protein at 25 °C, which can be used[32] to assess whether the slow- or the fast-exchange regime applies. For the signals at δ 11.8, 10.4 and 10.2 the significant slopes indicate the slow regime, whereas those at δ −1.1 and −2.4 are apparently in the fast regime. In the case of the slow-exchange regime the rate constants derived from the T_1 and T_2 data will be the same, and in the case of small differences the T_2 data will be the more correct. It is apparent that this condition is best met by the proton resonating at δ 10.4, and it is

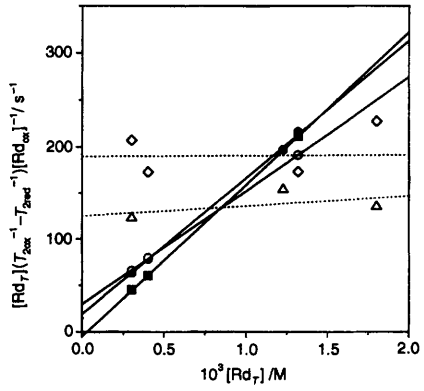

Fig. 8 Plots showing the variation of $[Rd_T](T_{2ox}^{-1} - T_{2red}^{-1})/[Rd_{ox}]$ against $[Rd_T]$ from NMR studies on the self-exchange of *C. pasteurianum* rubredoxin at 25 °C for peaks at δ 11.8 (■), 10.4 (●), 10.2 (○), −1.1 (△) and −2.4 (◆)

therefore concluded that the self-exchange rate constant is *ca.* 1.6×10^5 M^{-1} s^{-1} in wild-type Rd at 25 °C. It is also apparent that the k_{ese} determined from the peak at δ 10.4 increases with temperature, as expected for the slow-exchange regime. For the Val8Glu variant the most reliable value of k_{ese} is also that derived from the peak at δ 10.4 and is 4.7×10^3 M^{-1} s^{-1}, although in this case the evidence for the slow-exchange regime is somewhat less compelling.

As an alternative to the foregoing approach the behaviour of a resonance at δ −1.11 in the reduced wild-type protein was also considered. This broadens and moves to δ −1.19 in the fully oxidised form, and the spectra of intermediate mixtures show excess broadening of up to 10 Hz attributed to the electron exchange according to equation (3), which applies to

$$\Delta\nu_{mix} = f_{red}\Delta\nu_{red} + f_{ox}\Delta\nu_{ox} + 4f_{red}{}^2f_{ox}{}^2\pi(\delta\nu)^2(\tau_{red} + \tau_{ox}) \quad (3)$$

rates of exchange faster than those required to give coalescence.[33] In this equation f_i is the molar fraction of i, $\Delta\nu_i$ is the half-height width of the resonance from i, $\delta\nu$ is the chemical shift difference in Hz between the oxidised and reduced forms, and τ_i is the lifetime of i. Hence in principle τ_i and k can be deduced without assumptions regarding the exchange regime.

In practice it was found that the observed chemical shift in mixtures was not a linear function of the proportions of oxidised and reduced forms, thus making it impossible to obtain a precise value for δν pertaining to a particular mixture. The effect of this difficulty is compounded by the dependence on $(\delta\nu)^2$ of equation (3). Furthermore, in the mixture the observed line showed significant asymmetry, perhaps owing to the presence of an overlapping peak and this significantly

Table 4 Calculated self-exchange rate constants k_{ese} (25 °C) for rubredoxin from studies (A) of the *P. aeruginosa* azurin ACu^{II} oxidation of Rd_{red}, and (B) of the *P. aeruginosa* cytochrome c_{551} Fe^{III} oxidation of Rd_{red}, at pH 7.0 (20 mM Tris–HCl), $I = 0.100$ M (NaCl)

(A)	$10^6[Rd_{red}]$/M	$10^5[ACu^{II}]/M^{-1}\ s^{-1}$	$10^{-6}k_{12}/M^{-1}\ s^{-1}$	$k_{ese}{}^a/M^{-1}\ s^{-1}$	$k_{ese}{}^b/M^{-1}\ s^{-1}$
	1.23	1.25	4.0	54	104
	1.89	1.93	4.1	57	109
	3.39	3.20	4.8	78	150
	6.00	6.25	4.6	71	138
	2.10[c]	2.12	4.1	70[d]	
(B)	$10^5[Rd_{red}]$/M	$10^6[Cyt\ c_{551}]$/M	$10^{-6}k_{12}/M^{-1}\ s^{-1}$	$k_{ese}{}^a/M^{-1}\ s^{-1}$	$k_{ese}{}^b/M^{-1}\ s^{-1}$
	0.50	0.50	3.2	16	31
	0.67	0.94	3.5	19	37
	1.00	1.00	3.1	15	29
	1.50	1.52	3.4	18	35
	0.55[c]	0.57	6.8	69[d]	

[a] Using −81 mV for Rd_{ox}–Rd_{red} couple. [b] Using −57 mV for Rd_{ox}–Rd_{red} couple. [c] Val8Glu variant of Rd. [d] Using −73 mV for Rd_{ox}–Rd_{red} couple of the Val8Glu variant.

affected the measurement of $\delta\nu_{mix}$. Depending upon the assumptions made regarding these two factors a 50:50 mixture of oxidised and reduced protein yielded values of k ranging from 9×10^4 to 3.6×10^5 $M^{-1}\ s^{-1}$. This range includes the value of 1.6×10^5 $M^{-1}\ s^{-1}$ found from the signal at δ 10.4 and thus the two approaches are in reasonable agreement.

In view of the uncertainty regarding the identification of the slow regime it might be supposed that the line broadening of the peak at δ −1.11 would yield the more reliable result. In fact, owing to the uncertainties referred to above this is not so, and it is clear that in such studies each case must be treated on its own merits.

Cross-reaction studies with azurin and cytochrome c_{551}

These two redox reactions can be summarised by equation (4), where azurin ACu^{II} was in ≥ten-fold excess, and equation (5)

$$Rd_{red} + ACu^{II} \longrightarrow Rd_{ox} + ACu^{I} \quad (4)$$

$$Rd_{red} + CytFe^{III} \longrightarrow Rd_{ox} + CytFe^{II} \quad (5)$$

with cytochrome c_{551} in the Fe^{III} form, where Rd_{red} was in ≥ten-fold excess. Rate constants k_{12} (25 °C) were determined at pH 7.0 from absorption changes at 490 and 417 nm for equations (4) and (5). Table 4 lists relevant data which were analysed using the Marcus equations (6) and (7),[34] where the

$$k_{12} = (k_{11}k_{22}K_{12}f)^{\frac{1}{2}} \quad (6)$$

$$\log f = (\log K_{12})^2/4 \log (k_{11}k_{22}/Z^2) \quad (7)$$

self-exchange rate constant k_{11} is for the azurin Cu^{I}–Cu^{II} exchange (7.5×10^5 $M^{-1}\ s^{-1}$),[32] or cytochrome c_{551} Fe^{II}–Fe^{III} exchange (4.6×10^6 $M^{-1}\ s^{-1}$),[35] and k_{22} is for Rd_{red}–Rd_{ox} (k_{ese} in this paper). The equilibrium constants K_{12} for the cross-reactions were obtained from reduction potentials, and the collision frequency Z is $\approx 10^{11}$ $M^{-1}\ s^{-1}$. At pH 7.0 reduction potentials *vs.* NHE are for the azurin Cu^{II}–Cu^{I} couple 308 mV,[36] the cytochrome c_{551} Fe^{III}–Fe^{II} couple 276 mV [37] and the rubredoxin Rd_{ox}–Rd_{red} couple −81 mV (this work). Results obtained are listed in Table 4. Self-exchange rate constants k_{ese} calculated for the Rd_{red}–Rd_{ox}, reaction are 54 ± 9 $M^{-1}\ s^{-1}$ (azurin) and 15.9 ± 2.0 $M^{-1}\ s^{-1}$ (cytochrome c_{551}). Using the previous $E^{\circ\prime}$ value (−57 mV)[9] for the Rd_{ox}–Rd_{red} couple there are only small changes in k_{ese} values. From less extensive studies on the Val8Glu variant, Table 4, k_{ese} values of 70 $M^{-1}\ s^{-1}$ (azurin) and 69 $M^{-1}\ s^{-1}$ (cytochrome c_{551}) were obtained at pH 7.0 with $E^{\circ\prime}$ as reported in Table 1 (−73 mV). No variations in kinetic behaviour[15] or reduction potentials, Table 1, are observed for Rd over the range pH 6.5–7.0, Table 1, and the k_{ese} values obtained indicate little or no effect of the amino acid change at position 8.

Discussion

Electron self-exchange rate constants k_{ese} for Rd_{red}–Rd_{ox} have been determined for the first time by direct measurement using NMR methods at 25 and 35 °C. Although few NMR peak assignments are available for Rd,[31] this has not prevented the use of unassigned signals such as those at δ 10.4 and 10.2 to study the electron self-exchange process. The resonance at δ 200 is known to be from a cysteine co-ordinated to the iron,[31] and in principle might therefore have been associated with the slow-exchange regime. Unfortunately, it was apparent from our experiments that ($T_{iox}^{-1} - T_{ired}^{-1}$) was too small for this to be the case. The value obtained for the rate constant k_{ese} at 25 °C is 1.6×10^5 $M^{-1}\ s^{-1}$, which is comparable to k_{ese} values for six Type 1 Cu proteins (10^3–10^6 $M^{-1}\ s^{-1}$). The latter have been the subject of a recent appraisal,[19] when a common mechanism involving interaction of the hydrophobic regions close to the active sites and containing the partially exposed co-ordinated histidine has been proposed. Such a hydrophobic–hydrophobic interaction is preferable to alternatives involving two acidic patches or a hydrophobic and acidic interaction *etc.* which in energetic terms are less acceptable.[19] Examination of the *C. pasteurianum* Rd_{ox} structure [10] by molecular graphics indicates that the nearest surface to the $Fe(Cys)_4$ active site is also substantially hydrophobic, and a similar involvement of two hydrophobic surfaces is proposed for self-exchange. Moreover two of the co-ordinated cysteines are partially exposed and a part of this surface. Consideration of such an interaction allows the closest possible bimolecular Fe–Fe approach. The distance of the Fe from the surface is ≈6 Å,[10] and without H_2O molecules interceding the closest approach of the two molecules is therefore ≈12 Å.

To test further this possibility the Val8Glu variant was used to study the effect on reactivity of inserting a negatively charged residue in the adjacent hydrophobic region. The position of residue 8 adjacent to the two surface-exposed cysteines is indicated in Fig. 9. Electrochemical measurements on wild-type Rd give no dependence of $E^{\circ\prime}$ on pH, Table 1. In the case of the Val8Glu variant $E^{\circ\prime}$ values are pH dependent, Fig. 3, and acid dissociation, pK_a, values for the glutamic acid in Rd_{red} (6.2) and Rd_{ox} (5.8) were obtained. The unusually high pK_a values are accounted for by retention of undissociated glutamic acid to higher pH's as a result of the hydrophobic character of the region. The higher pK_a for Rd_{red} is as expected in view of the smaller charge on the Fe. A similar high value has been

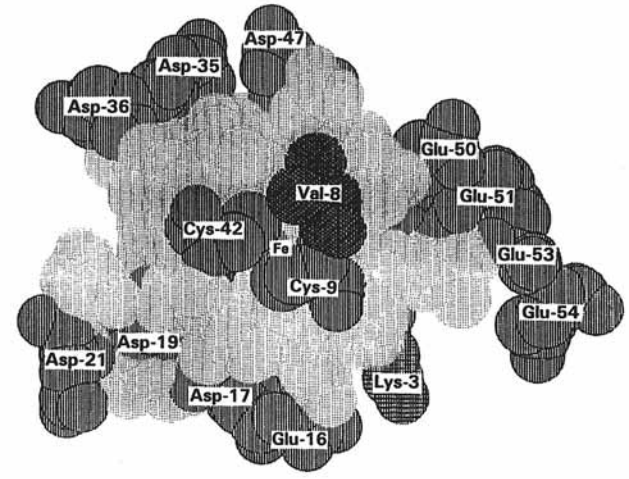

Fig. 9 Space-filling model showing the surface-exposed Cys-9 and Cys-42 residues which are co-ordinated to the Fe, and the close proximity of Val-8 in the hydrophobic region

observed for the glutamic acid of the Leu12Glu variant inserted in the hydrophobic region of PCu^{I} plastocyanin, pK_a 6.9.[38] At pH 6.5 negatively charged glutamate is dominant for both the Rd_{red} and Rd_{ox} variant forms, and the 34-fold decrease in k_{ese} to 4.7×10^3 M^{-1} s^{-1} confirms this region as relevant to the self-exchange process. A similar effect has been observed with azurin, when the insertion of charge Met44Lys into the hydrophobic region decreases k_{ese} by about the same factor.[24]

Values of k_{ese} for Rd have also been determined by cross-reaction studies with azurin ACu^{II} and cytochrome c_{551} Fe^{III} in turn as oxidant for Rd_{red}. Here the two k_{ese} values (54 and 15.9 M^{-1} s^{-1} averaging 35 M^{-1} s^{-1}) are in close agreement, but differ by $>10^3$ from the NMR value. Moreover the Val8Glu variant has only a small effect (< factor of 2) on both reactions at pH 7.0. A difference of this magnitude in k_{ese} suggests that ACu^{II} and cytochrome c_{551} Fe^{III} use an alternative site for electron transfer on Rd_{red}. Whether this is physiologically relevant remains to be established.

Cross-reaction rate constants for the reaction of rubredoxin and $[Ru(NH_3)_6]^{2+/3+}$ have been shown to be in error by $\times 34$,[39] and the rubredoxin k_{ese} value of $\approx 10^9$ M^{-1} s^{-1} no longer applies therefore. The correction factor here translates into a $\approx 10^3$ smaller k_{ese} taking into account the square-root dependence in the Marcus equation, giving k_{ese} in satisfactory agreement with that from NMR measurements of 1.6×10^5 M^{-1} s^{-1}. The latter can be compared to k_{ese} values for the higher plant plastocyanins, *e.g.* spinach and parsley, which are in the range (3–4) $\times 10^3$ M^{-1} s^{-1}.[19b] An important limiting factor in the case of the plastocyanins is the overall charge on the reactants (−9 and −8), even though exchange occurs *via* a hydrophobic–hydrophobic surface interaction.[19b] Another highly charged protein self-exchange reaction is that between the Fe^{II} and Fe^{III} cytochrome c (+7 and +8), when k_{ese} is $\approx 2 \times 10^3$ M^{-1} s^{-1}.[40] Rubredoxin is also highly charged suggesting that other factors may contribute to the 10^2 larger k_{ese}. In their discussion of the earlier rubredoxin k_{ese} of 10^9 M^{-1} s^{-1} Solomon and co-workers[41] drew attention to metal–S(Cys) bond lengths in Rd_{ox}(Fe–S 2.26 Å), as compared to that for plastocyanin (Cu^{II}–S 2.13 Å),[42] and suggested that the lack of π bonding in the former case is important, a point which may still be valid in explaining the now much smaller difference in k_{ese}.

In conclusion this work provides the first direct experimental determination of k_{ese} (1.6×10^5 M^{-1} s^{-1}) at 25 °C for the Rd_{red}–Rd_{ox} exchange. Electron exchange *via* the adjacent hydrophobic surfaces (Fe–Fe separation ≈ 12 Å) is supported by experiments using the adjacent Val8Glu variant, when for the glutamate form (pH 6.5) k_{ese} decreases to 4.7×10^3 M^{-1} s^{-1}. An earlier estimate of k_{ese} from cross-reaction studies 10^9 M^{-1} s^{-1} has been shown to be in error.[39] Cross-reaction studies with azurin and cytochrome c_{551} as oxidants for Rd_{red} suggest an alternative site for electron transfer with $k_{ese} \approx 35$ M^{-1} s^{-1}. Such an assignment is supported by studies with Val8Glu, which have little (< two-fold) effect on this k_{ese}.

Acknowledgements

We are grateful to Dr. J.-M. Moulis for supplies of proteins, and to the British Council for their generous support (to S.-C. I.), and travel under the Alliance Scheme (S.-C. I. and H.-Y. Z.-J.). We are also grateful to the Leverhulme Trust for a Fellowship (to W. McF.).

References

1 See, for example, W. A. Eaton and W. Lovenberg, in *Iron-Sulfur Proteins*, ed. W. Lovenberg, Academic Press, New York, 1973, vol. 2, pp. 131–160.
2 L. H. Jensen, in *Iron-Sulfur Protein Research*, Japan Scientific Societies Press, Osaka, 1987, pp. 3–21.
3 C. D. Stout, in *Iron-Sulfur Proteins*, ed. T. Spiro, Wiley-Interscience, New York, 1982, vol. 4, pp. 97–146.
4 L. C. Sieker, R. E. Tenkamp and J. LeGall, *Methods Enzymol.*, 1994, **243**, 203.
5 L. Chen, M.-Y. Liu, J. LeGall, P. Fiareleira, H. Santos and A. V. Xavier, *Biochem. Biophys. Res. Commun.*, 1993, **193**, 100.
6 L. Chen, M.-Y. Liu, J. LeGall, P. Fiareleira, H. Santos and A. V. Xavier, *Eur. J. Biochem.*, 1993, **216**, 443.
7 H. Santos, P. Fiareleira, A. V. Xavier, L. Chen, M.-Y. Liu and J. LeGall, *Biochem. Biophys. Res. Commun.*, 1993, **195**, 551.
8 J. Peterson, M. Kusunose, E. Kusunose and M. T. Coon, *J. Biol. Chem.*, 1967, **242**, 4334; G. Eggink, H. Engel, G. Vriend, P. Terpstra and B. Witholt, *J. Mol. Biol.*, 1990, **212**, 135.
9 W. Lovenberg and B. E. Sobel, *Proc. Natl. Acad. Sci. USA*, 1965, **54**, 193.
10 K. D. Watenpaugh, L. C. Sieker and L. H. Jensen, *J. Mol. Biol.*, 1979, **131**, 159.
11 E. T. Adman, L. C. Sieker and L. H. Jensen, *J. Mol. Biol.*, 1991, **217**, 337; 1980, **138**, 615.
12 M. Frey, L. C. Sieker, F. Payan, R. Haser, M. Bruschi, G. Pepe and J. LeGall, *J. Mol. Biol.*, 1987, **197**, 525.
13 E. R. Stenkamp, L. C. Sieker and L. H. Jensen, *Proteins: Struct., Funct., Genet.*, 1990, **8**, 352.
14 M. W. Day, B.-T. Hsu, L. Joshua-Tor, J.-B. Park, Z.-H. Zhou, M. W. W. Adams and D. C. Rees, *Protein Sci.*, 1992, **1**, 1494.
15 C. A. Jacks, L. E. Bennett, W. N. Raymond and W. Lovenberg, *Proc. Natl. Acad. Sci. USA*, 1974, **4**, 1118.
16 L. E. Bennett, in *Iron-Sulfur Proteins*, Academic Press, New York, 1977, vol. 3, pp. 331–379.
17 R. G. Shulman, P. Eisenberger, B.-K. Teo, B. M. Kincaid and G. S. Brown, *J. Mol. Biol.*, 1978, **124**, 305.
18 R. W. Lane, J. A. Ibers, R. B. Frankel, G. C. Papaefthymiou and R. H. Holm, *J. Am. Chem. Soc.*, 1977, **99**, 84.
19 (*a*) C. Dennison, T. Kohzuma, W. McFarlane, S. Suzuki and A. G. Sykes, *J. Chem. Soc., Dalton Trans.*, 1994, 437; (*b*) P. Kyritsis, C. Dennison, W. J. Ingledew, W. McFarlane and A. G. Sykes, *Inorg. Chem.*, 1995, **34**, 5370.
20 R. K. Gupta, *Biochim. Biophys. Acta*, 1973, **292**, 291; D. W. Dixon, X. Hong and S. E. Woehler, *Biophys. J.*, 1989, **56**, 339; D. W. Dixon, X. Hong, S. E. Woehler, A. G. Mauk and B. P. Sishta, *J. Am. Chem. Soc.*, 1990, **112**, 1082.
21 I. Bertini, A. Gaudemer, C. Luchinat and M. Piccioli, *Biochemistry*, 1993, **32**, 12887.
22 Y. Pétillot, E. Forest, I. Mathieu, J. Meyer and J.-M. Moulis, *Biochem. J.*, 1993, **296**, 657.
23 J. Meyer, J. Fujinaga, J. Gaillard and M. Lutz, *Biochemistry*, 1994, **33**, 13642.
24 M. Van de Kamp, R. Floris, F. C. Hali and G. W. Canters, *J. Am. Chem. Soc.*, 1990, **112**, 907.
25 A. F. W. Coulson and R. C. I. Oliver, *Biochem. J.*, 1979, **181**, 189.
26 L.-C. Tsai, L. Sjölin, V. Langer, T. Pascher and H. Nar, *Acta Crystallogr., Sect. D*, 1995, **51**, 168; W. E. B. Shepard, B. F. Anderson, D. A. Lewandoski, G. E. Norris and E. N. Baker, *J. Am. Chem. Soc.*, 1990, **112**, 7817; Y. Matsuura, T. Takano and R. E. Dickerson, *J. Mol. Biol.*, 1982, **156**, 309.
27 L.-H. Guo and H. A. O. Hill, *Adv. Inorg. Chem.*, 1991, **36**, 341.

28 I. Quinkal, V. Davasse, J. Gaillard and J.-M. Moulis, *Protein Eng.*, 1994, **7**, 681.
29 A. C. McLaughlin and J. S. Leigh, *J. Magn. Reson.*, 1973, **9**, 296.
30 P. L. Dutton, *Methods Enzymol.*, 1978, **54**, 411.
31 B. Xia, W. M. Westler, H. Cheng, J. Meyer, J.-M. Moulis and J. L. Markley, *J. Am. Chem. Soc.*, 1995, **117**, 5347.
32 (*a*) C. M. Groeneveld, M. C. Ouwerling, M. C. Erkelens and G. W. Canters, *J. Mol. Biol.*, 1988, **200**, 189; (*b*) C. M. Groeneveld and G. W. Canters, *J. Biol. Chem.*, 1988, **263**, 167.
33 S. Meiboon, Z. Luz and D. Gill, *J. Chem. Phys.*, 1957, **27**, 1411.
34 R. A. Marcus and N. Sutin, *Biochim. Biophys. Acta*, 1985, **811**, 265.
35 R. Timkovich and M. L. Cai, *Biochem. Biophys. Res. Commun.*, 1985, **150**, 1044.
36 T. Pascher, G. Karisson, M. Nordling, B. G. Malmström and T. Vänngård, *Eur. J. Chem.*, 1993, **212**, 289.
37 V. T. Toniguchi, N. Sailasuta-Scott, F. C. Anson and H. B. Gray, *Pure Appl. Chem.*, 1980, **52**, 2275.
38 P. Kyritsis, C. Dennison, W. McFarlane, M. Nordling, T. Vänngård, S. Young and A. G. Sykes, *J. Chem. Soc., Dalton Trans.*, 1993, 2289.
39 S.-C. Im and A. G. Sykes, *J. Chem. Soc., Dalton Trans.*, 1996, 2219.
40 R. K. Gupta, S. H. Koenig and A. G. Redfield, *J. Magn. Reson.*, 1972, **7**, 66.
41 M. D. Lowery, J. A. Guckert, M. S. Gebhard and E. I. Solomon, *J. Am. Chem. Soc.*, 1993, **115**, 3012.
42 See, for example, A. G. Sykes, *Adv. Inorg. Chem.*, 1991, **36**, 384.

Received 22*nd July* 1996; *Paper* 6/05076J